IBRACON Structures and Materials Journal
Revista IBRACON de Estruturas e Materiais

ORIGINAL ARTICLE

Numerical analyses of two-pile caps considering lateral friction between the piles and soil

Análise numérica de blocos sobre duas estacas considerando o atrito lateral entre as estacas e solo

Rodrigo Gustavo Delalibera[a] 🆔
Gabriel Fernandes Sousa[a] 🆔

[a]Universidade Federal de Uberlândia – UFU, Faculdade de Engenharia Civil, Uberlândia, MG, Brasil

Abstract: Pile caps are structural elements used to transfer loads from the superstructure to a group of piles. The design of caps is normally based on analytical formulations, considering the strut and tie method. Through the advance of computational technology, the use of an integrated soil and foundation model may suggest a behavioral trend to obtain a more realistic modeling for the structural element being studied. This work aimed at analyzing, in numerical fashion, the structural behavior of reinforced concrete two-pile caps considering the lateral friction between the piles and the ground through a continuous modeling, as well as to analyze the portion of the load that is transferred to the ground directly by the cap. The lateral friction was modeled considering node coupling and through contact elements. Simulations were performed considering three soil types (sandy, clayish, and soilless), three cap heights, and three pile lengths. Soil parameters were obtained through semi-empirical correlations. Through these analyses, the conclusion was reached that, on average, 4.50% of the force applied to the pillar is transferred directly to the ground by cap. In terms of the principal compression stresses, in the superior nodal region, the strut tends to form beyond the section of the column. Alternatively, increasing cap stiffness provided, on average, an increase in the load carrying capacity of the models.

Keywords: pile caps, reinforced concrete, soil, lateral friction, numerical analysis.

Resumo: Blocos sobre estacas são elementos estruturais usados para transferir ações da superestrutura para um conjunto de estacas. O dimensionamento de blocos é comumente realizado por meio de formulações analíticas, considerando-se o método de bielas e tirantes. Com o avanço da tecnologia computacional, a utilização de um modelo integrado, considerando a influência do solo e da rigidez das estacas, poderá surgir uma tendência de comportamento de modo a se obter uma modelagem mais próxima do comportamento real dos blocos. Este trabalho teve como objetivo analisar por meio de análises numéricas o comportamento estrutural de blocos de concreto armado sobre duas estacas, considerando o atrito lateral entre as estacas e o solo por meio de uma modelagem contínua, bem como analisar a parcela de força transferida ao solo diretamente através da base do bloco. O atrito lateral foi modelado considerando o acoplamento de nós e por meio de elementos de contato. Assim, foram realizadas simulações considerando três configurações: solo arenoso, solo argiloso e sem solo, três alturas de bloco e três comprimentos de estaca. Os parâmetros do solo, como módulo de elasticidade, ângulo de atrito e coeficiente de Poisson foram obtidos através de correlações semiempíricas, baseadas em ensaios de percussão simples. Constatou-se que, em média, 4,50% das forças aplicadas no pilar são transferidas diretamente ao solo por meio da base do bloco. Com relação às tensões principais de compressão, verificou-se que na região nodal superior, a biela tende a se formar além da seção do pilar. Já o aumento da rigidez do bloco proporcionou, em média, um aumento da capacidade portante dos modelos.

Palavras-chave: blocos sobre estacas, concreto armado, atrito lateral, análise numérica.

1 INTRODUCTION

The act of determining the type of foundation to be used in a construction is realized through technical studies, the main purpose behind these studies is to analyze the characteristics of the soil in terms of its load capacity and compressibility of the soil, along with the condition of the foundations of the neighboring buildings, as well as economic factors. Therefore, knowledge regarding soil parameters, the intensity of the forces that will be distributed through it, along with an understanding of the building limits, allows one can choose the type of foundation most suitable for a given construction.

There are situations in which the superficial layers of the soil do not have sufficient support capacity to absorb and distribute the forces arising from the superstructure. In such cases, it is necessary to use one of the deep foundation types.

It is understood that deep foundations are those that transmit the load to the soil through its base or through lateral friction, these being the piles and the caissons. The choice of foundation, however, requires the construction of structural elements - the pile cap.

According to NBR 6118 [1], pile caps are volume structures used to transmit foundation loads to the piles. Therefore, it can be said that all external dimensions have the same order of magnitude. These are treated as special structural elements, which do not respect the hypothesis that the flat sections remain flat after deformation, as these are not long enough for localized disturbances to dissipate.

1.1 Justification

The present research is justified through the importance that pile caps have in the structure of a building, as well as through the limited amount of research, in the literature, with numerical emphasis, which is directed toward the analysis of the integrated behavior associated with the pile cap-pile-soil set by the adoption of contact elements. The contact between the crown block and the soil promotes the transfer of a portion of the load directly to the soil, where there is not a total transfer of the force acting on the column onto the top of the piles. Taking the aforementioned into consideration, this study becomes of importance since the integrated analysis allows for the quantification of portions linked to the vertical force transferred directly to the soil through the block. In addition, the calculation methods used for the design of pile blocks do not cogitate the presence of soil, and as such do not deliberate on the variation in the stress field that occurs due to the direct contact between the structural elements and the soil.

1.2 Objective

This study aims at analyzing, through numerical modeling, the structural behavior of foundation blocks on two precast reinforced concrete piles, while allowing for the friction between the pile and the soil, by knot coupling (perfect stiffness) and by contact elements. Through a joint modeling (pile cap-pile-soil), an analysis of variance (ANOVA) was carried out, generating through such the study of the behavioral tendency associated with the bearing capacity of the models, and the portion of force transferred directly to the soil through the pile cap. Finally, an attempt was made at verifying whether there exists agreement between the pile repression in the numerical models studied with the repression obtained analytically.

2 DESIGN OF THE MODELS

Pile caps were analyzed on two piles, these were subjected to centered force loads, varying the following parameters: pile cap height (28 cm, 50 cm, and 70 cm), pile length (5 m, 7 m and 9 m), soil type (sand, clay and without soil), under conditions where bonding between the structure and the soil occurs (knot coupling and contact element). Figure 1 presents the geometries of the analyzed models and their conditions. In total 45 pile caps were modeled on two piles and numerical modeling was performed with the aid of a computational tool based on the finite element method - FEM.

As shown in Figure 2, the strength of 25 MPa and 50 MPa for the concrete in the pile caps, columns and piles was adopted, since the study dealt with the analysis of the bearing capacity of the pile caps. For steel bars, the NBR 6118 criterion [1] was used, admitting a perfect elastoplastic behavior for steel, with yield strength of 500 MPa.

The piles caps were checked and dimensioned using the strut and tie model, according to the criteria of Blévot and Frémy [2].

Noted herein was for the proposed block heights, the limit of the angle of inclination for the compression rod recommended by Blévot and Frémy [2], to guarantee rigidity of the pile cap ($45^\circ \leq \theta \leq 55$), was not met for the models with

height of 28 cm and 70 cm. However, the recommendations of NBR 6118 [1] were met, which suggests that the tangent of the compressed diagonal angle is between 0.57 (29.7º) and 2 (63.4º). This information can be found on Table 1.
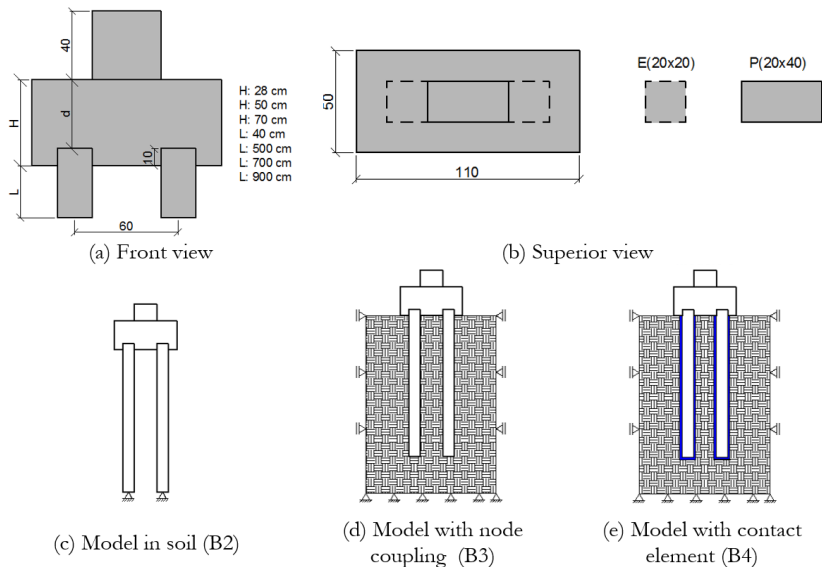

Figure 1. Characteristics of the models analyzed in the research (measured in centimeters).
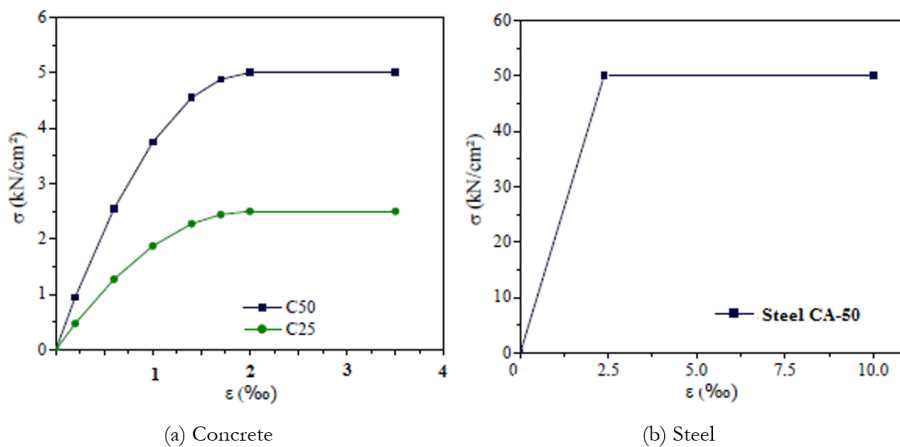

Figure 2. Material constitutive model: concrete and steel.

Regarding the dimensioning of column and pile reinforcement, the criteria of NBR 6118 [1] were considered. For the pile caps, only the existence of the main tensile reinforcement (tie) was considered. The quantity of steel bars for each structural element is provided on Table 2. Here A_{st} is the main reinforcement of the pile cap, A_{sp} the longitudinal reinforcement of the column and A_{se} the longitudinal reinforcement of the piles.

Table 1 - Inclination of strut according to pile cap height.

Model height	Column	θ (degrees)	Useful height (cm)	Load
H28		30.96	18	
H50	20 x 40	53.13	40	Vertical e Centered
H70		63.4	60	

Table 2 - Quantitative reinforcement for structural elements

Model	A_{st}	A_{sp}	A_{se}
B2P40H28e0			
B3P40H28e0	3 ø 20 mm	6 ø 10 mm	4 ø 10 mm
B4P40H28e0			
B2P40H50e0			
B3P40H50e0	5 ø 16 mm	6 ø 12.5 mm	4 ø 10 mm
B4P40H50e0			
B2P40H70e0			
B3P40H70e0	4 ø 16 mm	8 ø 12.5 mm	4 ø 12.5 mm
B4P40H70e0			

3 NUMERIC MODELING

For modeling of the piles and columns, the ANSYS® computer program [3] was used. The concrete behavior was simulated using two constitutive models. For stress simulation, the CONCRETE model was used, which is based on the Willam-Warnke model [4], where it was possible to simulate cracked concrete when subjected to tensile stresses that exceed the pre-established limit. In the CONCRETE model, it is necessary to provide parameters such as the shear transfer coefficient through an open crack (βa), shear transfer coefficient through a closed crack (βf), ultimate tensile strength and ultimate compressive strength. However, as the compression behavior of the concrete will be modeled according to the Von Mises criterion (simulating the plasticization of the concrete), it is necessary to disable the compressive strength in the CONCRETE model, adopting the value of -1 for this parameter.

To quantify the ultimate tensile strength, the NBR 6118 criterion [1] was used, according to Equation 1.

$$f_{ct,m} = 0.3 \cdot f_{ck}^{2/3} \tag{1}$$

In Equation 1, f_{ck} is the characteristic compressive strength of concrete and $f_{ct,m}$ the average tensile strength of concrete, both expressed in MPa.

The behavior of concrete in compression was simulated according to the Multilinear model available in the Ansys® library [3], following the Von-Mises criterion. This criterion was used to improve the convergence of the models, since the CONCRETE model only presents numerical instability, which hinders convergence. The NBR 6118 stress-strain curve criteria were analyzed [1], along with the model proposed by Desay and Krishnan [5].

In Figure 2, the isotropic behavior of class C25 and C50 materials is established for block, column and pile respectively, in reference to the model proposed by NBR 6118 [1].

Regarding the shear transfer coefficients, Delalibera [6] used 1.0 for the βa and βf parameters, whereas Munhoz [7] suggests the use of 0.2 for βa and 0.6 for βf. In the present work, 0.2 was used for βa and 0.8 for βf, since a better convergence was noted with the use of such parameters.

For reinforcements, the Von-Mises plasticization criterion was considered, according to a perfect elasto-plastic model.

In the ANSYS® software [3], the simulation of the perfect elasto-plastic model is carried out using a bilinear isotropic model, where it is necessary to inform the steel elasticity module (E_s), the flow resistance (f_y) and the tangent elasticity module (ET). In the present work, CA-50 steel was used, with an elastic modulus of 210 GPa, yield strength of 500 MPa and the tangent modulus was null, as seen in Figure 2.

For the soil material, the Drucker-Prager model and the model representing elasto-plastic behavior were considered, where the flow is controlled by a combination of the hydrostatic stress and the deviation stress.

The concrete and soil elements were modeled with the finite element SOLID65. This element has eight nodes with three degrees of freedom per node - translations in the x, y and z directions. The element has plastic deformations, cracking and crushing in three orthogonal directions. In the SOLID65 element, cracking occurs when the main tensile stress in any direction reaches the breaking surface. After cracking, the modulus of elasticity of the concrete becomes equal to zero in the direction considered. Crushing occurs when the set of compressive stresses acting on the rupture planes exceeds the limit resistance established by a rupture surface, subsequently, the modulus of elasticity becomes equal to zero in all directions. The SOLID65 element is seen in Figure 3.
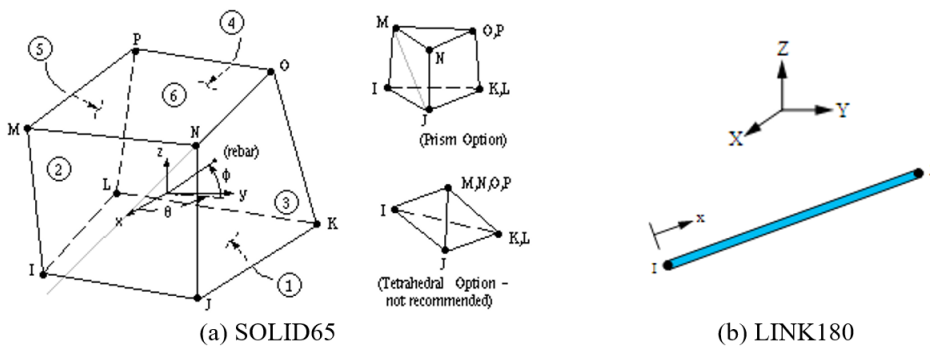
(a) SOLID65 (b) LINK180

Figure 3. Finite elements used in modeling concrete, soil and steel bars.

In modeling the steel bars of the armature, the finite element LINK180 was used (Figure 3).

This element has two nodes, each node possessing three degrees of freedom - translations in the x, y, and z directions. Therefore, this element was chosen, as the reinforcement in the models was considered to be discrete.

The friction between the piles and the soil was simulated by coupling the nodes (perfect friction) and by using finite contact elements. The contact surfaces between the materials were represented by two finite elements, in which the association of these elements, called "contact pair", is necessary to determine a contact surface and a target surface. For the contact surface (pile and block), the finite element CONTACT174 was used and for the target surface (soil), the finite element TARGET170 was used. These elements have three degrees of freedom on each node and the geometric properties are the same as the faces of the solid elements to which they are attached and may have triangular or quadrangular geometry. The finite elements CONTACT174 and TARGET170 are noted in Figure 4.
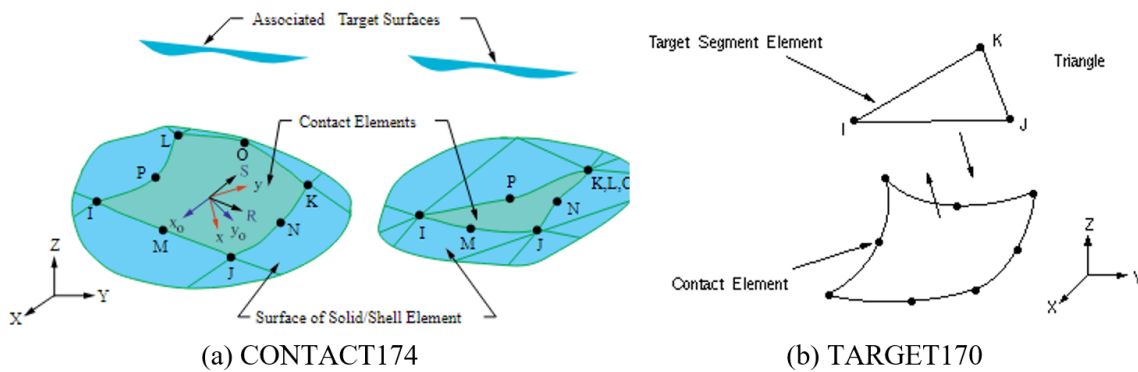

(a) CONTACT174 (b) TARGET170

Figure 4. Finite elements used to model contact elements.

The models were named according to the type of connection (B2, B3 and B4), to the cross-sectional dimension of the column (P40), to the height of the block (H28, H50, H70), to the length of the pile (L5, L7 and L9), to the soil type (S0, S1 and S2) and finally to the loading eccentricity (e0). As an example, the model B3P40H70L9S2e0 is a model in which we used node coupling as bonding, a 40 cm column in the transverse direction, a 70 cm high block, 900 centimeters piles, type 2 (clayish) soil and loading with zero eccentricity.

4 MEASURING OF THE MODELS

To verify which refinement is necessary for the finite element mesh, a mesh convergence test was carried out. Such a test is important so that the mesh used does not contain a very large quantity of elements, which would make the processing time impracticable. To perform this test, the B115P250R1 pile cap was used, tested experimentally by Munhoz [7]. Figure 5 shows the meshes used in the analysis. Emphasis is here placed on the different element division

sizes of 20 cm, 10 cm, 5 cm, 4 cm, 3 cm and 2.5 cm that were tested. Noteworthy here is that some elements presented non-standard values, since it was necessary to have divisions in the places where there are reinforcements.

As observed in Figure 6, verification is made into the incremental displacement history for each mesh. Through such, one notes that the mesh refinement reduced the linear phase of the material, as such producing the more recent cracks. However, with respect to the final displacement, convergence was identified at values close to 0.75 mm. Therefore, still in Figure 6, there is the convergence of the vertical displacement, according to the finite element mesh refinement. The meshes with 7920 elements, 9934 elements and 13570 elements showed very close displacements, confirming the tendency towards a convergence of behavior. As such, the conclusion was reached that a mesh with a division of approximately 3 cm led to an acceptable behavior trend, saving computational time for a mesh with more elements.

Figure 5. Finite element meshes tested.
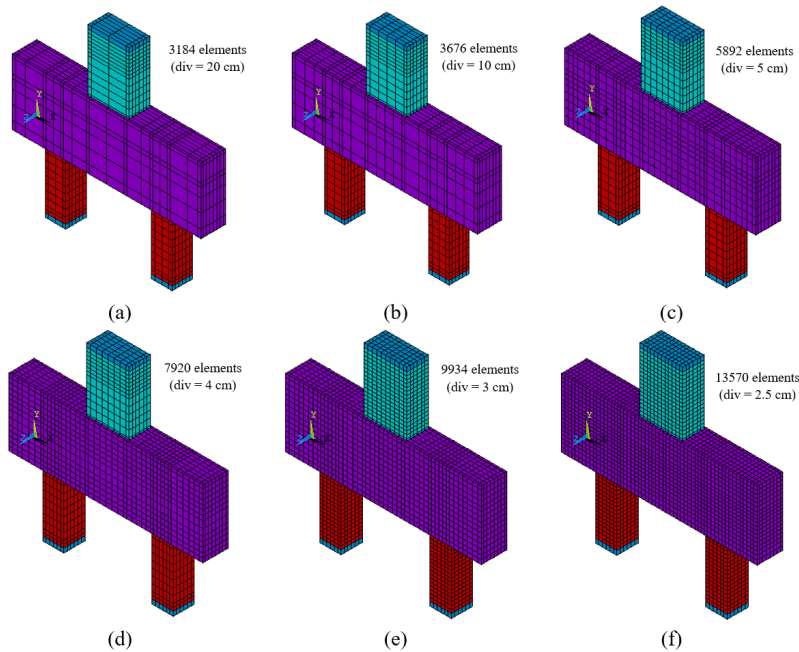
To validate the modeling criteria, a numerical result behavior test was performed, comparing it with experimental data. Block B115P250R1 was used, experimentally tested by Munhoz [7].
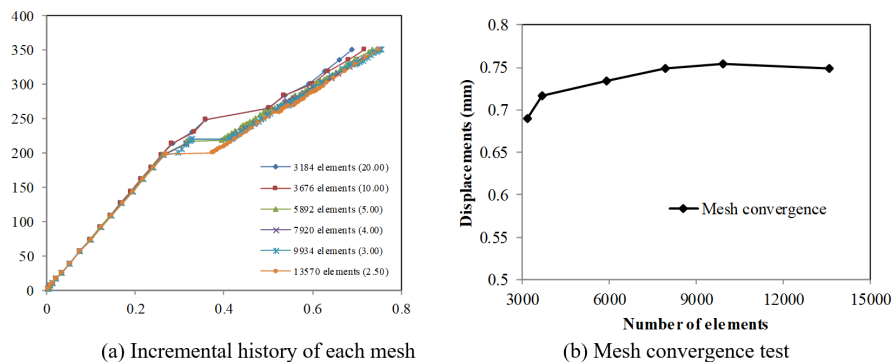

(a) Incremental history of each mesh   (b) Mesh convergence test

Figure 6. Convergence test of vertical displacement in the lower center of the pile cap according to mesh refinement.

In Figure 7, one notes the comparison between the Force-Displacement curves, which refers to the numerical and experimental models. The numerical models processed with the constitutive model CONCRETE (with experimental elasticity module) and Multilinear (according to the stress vs. concrete deformation curve calculated according to NBR 6118 [1]) were proven to be more rigid than the experimental model from Munhoz [7]. Therefore, a correction was made in the pile caps stiffness ($E_{cs} \cdot I$), modifying the pile caps elasticity module, with the intuition of making the model more flexible. The new modulus of elasticity was calculated based on Equation 2, taking into account the cracking of the block. The block was considered as a beam subjected to a concentrated force in the center of the span. Therefore, based on the displacement in which the first crack in the Munhoz block occurred [7], the corrected elastic modulus can be obtained.

$$E_{cor} = \frac{F \cdot L_{est}^{3}}{48 \cdot \delta \cdot I} \tag{2}$$

E_{cor} is the corrected elasticity module, Lest the distance between the pile axis, I the moment of inertia of the pile cap cross section, F the vertical force referring to the appearance of the first crack in the experimental model and δ the vertical displacement referring to the instant of the first fissure.

Elasticity modules with values of 3575.70 MPa, 4500 MPa and 6100 MPa were tested. The best approximation occurred with an Ecor of 6100 MPa. With the elasticity module corrected, the multilinear model proposed by Desay and Krishnan was tested [5]. As shown in Figure 7, this model led to an ultimate force of 770 kN, a force greater than that achieved only with the CONCRETE model.
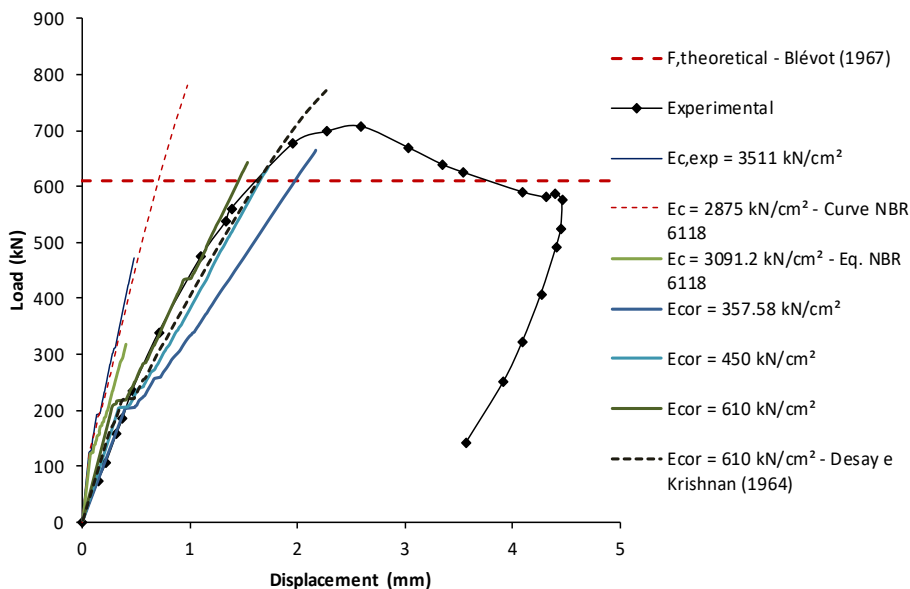

Figure 7. Calibration of the numerical model to Munhoz's experimental results [6].

The use of the Desay and Krishnan model [5] with $E_{cor} = 6100$ MPa led to a good approximation, producing in the model a higher carrying capacity than the model in which the CONCRETE criterion was used alone, for the same value of modulus of elasticity. The conclusion was reached, therefore, that the use of a Multilinear model associated with the CONCRETE model led to a better numerical representation of the Munhoz experimental model [7], being, therefore, the acceptable criteria for simulating the element. On Table 3, one can identify how the ultimate numerical strength ($F_{u,num}$) differs from the theoretical strength values (F_{Teo}), calculated according to the Blévot and Frémy model [2], and the ultimate experimental ($F_{u,exp}$), obtained experimentally.

With the numerical modeling at hand, the authors herein noted the cracking panorama, connecting rods and stress flow obtained for the numerical model with Ecor of 6100 MPa approached the Munhoz experimental result [7], as seen in Figure 8.

By producing the ratio between the corrected elasticity modulus and the real elasticity modulus of the structure, one obtains the reduction coefficient for the modulus of elasticity for the models of the present study, according to Equation 3.

Table 3 - Quantitative reinforcement for structural elements.

Modeling	F_{Teo} (kN)	$F_{u,exp}$ (kN)	$F_{u,num}$ (kN)	$F_{u,exp}/F_{u,num}$	$F_{Teo}/F_{u,num}$
Curve – NBR 6118 [1]			781.25	0.91	0.78
$E_{c,exp}$ = 3511 kN/cm^2			437.29	1.63	1.39
E_{cor} = 357.58 kN/cm^2			664.69	1.07	0.92
E_{cor} = 450 kN/cm^2	609.40	712.67	634.53	1.12	0.96
E_{cor} = 610 kN/cm^2			643.7	1.11	0.95
E_{cor} = 610 kN/cm^2 - Desay and Krishnan [4]			770	0.93	0.79

(a) Cracks – experimental Model f Munhoz [5]

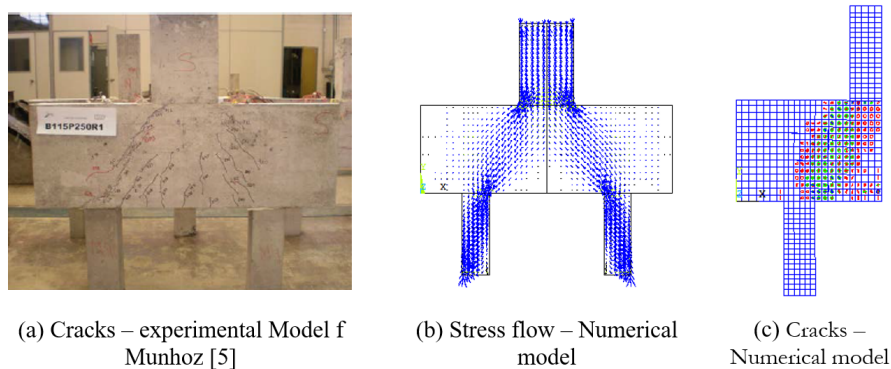(b) Stress flow – Numerical model

(c) Cracks – Numerical model

Figure 8. Conformity between the numerical model and the experimental model, through the stress flow and cracking pattern.

$$k_{red} = \frac{E_{cor}}{E_{c,exp}} = \frac{6100.00}{35110.00} = 0.174 \tag{3}$$

To assess the behavior of the contact elements, simulations were carried out, varying the normal contact stiffness (FKN) and analyzing how this would influence the maximum penetration, maximum pressure and number of iterations until convergence.

According to Silva [8], contact stiffness is inversely proportional to penetration. The author also states that, ideally, penetration should not occur between the bodies in contact with each other, as physically the bodies could not occupy the same position; however, numerical devices are commonly used in solutions of contact problems and allow for the existence of a small penetration, this penetration being defined according to a tolerance factor (FTLN).

The simulations were performed with a tolerance factor (FTLN) fixed at 10% in order to reduce the possibility of loss of stability of the finite element SOLID65. The hexahedral element of the soil in contact with the pile has a dimension of 50 cm while the hexagonal element of the pile has a maximum dimension of 5 cm. Therefore, when using a penetration tolerance factor FTOLN = 0.10, satisfactory results are those that lead to a maximum penetration equal to or less than 5 mm (5 cm × 0.10 = 5 mm). Therefore, as noted in Figure 9, the maximum penetration values are acceptable and tend to stabilize as the FKN factor increases.

All simulations were carried out for three coefficients of friction between the concrete and the soil (μ = 0.20; μ = 0.60; μ = 1.00), in order to analyze the behavior trend and verify how the analysis parameters behaved by stiffening the system. As noted from Figure 9, the reduction of the friction coefficient provided an increase in maximum penetration, by maintaining the penetration factor and by increasing the stiffness factor. However, although there is variation in penetration, the change in the friction coefficient was not seen as promoting significant variations in the

studied parameters and as the FKN value was added, the parameters analyzed (maximum penetration, maximum pressure, and total number of iterations) tended to match.

Noted by analyzing the contact pressure, seen in Figure 9, was that an initial variation, from 0.10 to 0.50, in the FKN factor promoted a significant drop (446%) in the average contact pressure, this being due to an increase in FKN, where a tendency towards stabilization was observed, as seen in Figure 9.

Finally, the number of iterations for the convergence of the results was analyzed, verifying that the increase in the stiffness factor FKN promoted an increase in the number of iterations, as shown in Figure 9, thus causing the problem to present greater convergence difficulties. After carrying out the analyses, the decision was reached to use in the simulations of the models the contact element, FKN = 15 and FTLN = 0.10. Regarding the friction coefficients, the requirements contained in NAVFAC [9] were followed, using for sandy soil, friction coefficient of 0.55 and for clay soil friction coefficient of 0.30. After the gauging tests and defining the characteristics of the numerical models, the parameters used to model the reinforced concrete structural elements are presented on Table 4.

Table 4 – Numerical parameters to modeling concrete and steel.

Material - Element	Linear properties	No-linear properties	
		Tension (CONCRETE)	
		$\beta a = 0.2$	
		$\beta f = 0.8$	
		$f_{ct} = 2.56$ MPa	
		Compression (multilinear isotropic)	
		Strain (‰)	Stress (MPa)
Pile Cap	$E_{cor} = 3915$ MPa	0	0
(SOLID65)	$\upsilon = 0.2$	0.0019157	7.50
		0.0032567	11.97
		0.0047893	16.44
		0.0058110	18.85
		0.0080000	22.49
		0.0100000	24.27
		0.0127714	25.00
		Tension and compression (CONCRETE)	
		$\beta a = 0.2$	
Piles e Column	$E_c = 39598$ MPa	$\beta f = 0.8$	
(SOLID65)	$\upsilon = 0.2$	fct = -1	
		fc = -1	
Steel (LINK180)	$E_s = 210000$ MPa	fy = 500 MPa	
	$\upsilon = 0.3$	Tangent module = 0	

In similar fashion to that presented for steel and concrete, Table 5 shows the soil analysis parameters used in the numerical models, showing the linear properties of each layer, as well as the Drucker-Prager model parameters.

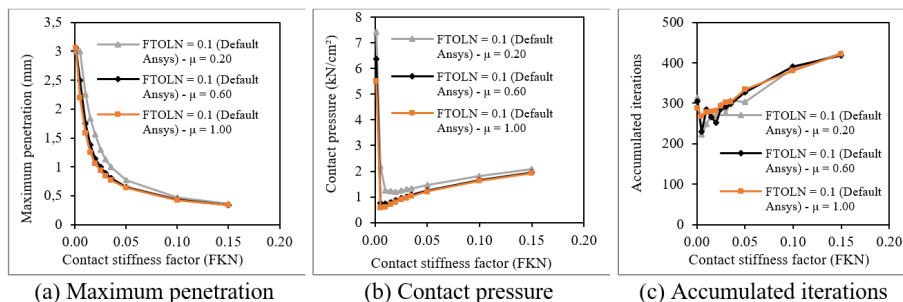(a) Maximum penetration   (b) Contact pressure   (c) Accumulated iterations

Figure 9. Calibration test of contact elements.

Table 5 – Numerical parameters for soil modeling - values obtained in the Technical Literature - Cintra and Aoki [10].

Layer	Element	Sandy soil Properties			Clay soil properties		
-1		E_{solo}=5.4MPa	Drucker-Prager		E_{solo}=2.8MPa	Drucker-Prager	
		$\upsilon = 0.30$	c=3.5kPa	$\phi = 21.2$ °	$\upsilon = 0.24$	c=17.5kPa	ϕ=17.5 °
-2		E_{solo} =13.5MPa	Drucker-Prager		E_{solo}=7 MPa	Drucker-Prager	
		υ =0.29	c=3.5kPa	$\phi = 25.00$ °	υ =0.23	c=17.5kPa	ϕ=17.5 °
-3		E_{solo} =27MPa	Drucker-Prager		E_{solo}=14 MPa	Drucker-Prager	
		$\upsilon = 0.28$	c=7.5kPa	$\phi = 29.14$ °	$\upsilon = 0.22$	c=37.5kPa	ϕ=20 °
-4		E_{solo} =35.1MPa	Drucker-Prager		E_{solo}=18.2MPa	Drucker-Prager	
		υ =0.28	c=15 kPa	$\phi = 31.12$ °	υ =0.21	c=75 kPa	$\phi = 25$ °
-5	SOLID 65	E_{solo}=51.3MPa	Drucker-Prager		E_{solo}=26.6 MPa	Drucker-Prager	
		υ =0.27	c=15 kPa	$\phi = 34.49$ °	υ =0.21	c=75 kPa	$\phi = 25$ °
-6		E_{solo} =62.1MPa	Drucker-Prager		E_{solo}=32.2MPa	Drucker-Prager	
		$\upsilon = 0.27$	c=30 kPa	$\phi = 36.45$ °	$\upsilon = 0.21$	c=150kPa	$\phi = 30$ °
-7		E_{solo} =75.6MPa	Drucker-Prager		E_{solo}=39.2MPa	Drucker-Prager	
		$\upsilon = 0.27$	c=30 kPa	$\phi = 38.66$ °	υ =0.21	c=150kPa	$\phi = 30$ °
-8		E_{solo} =94.5MPa	Drucker-Prager		E_{solo} = 49 MPa	Drucker-Prager	
		$\upsilon = 0.27$	c=30 kPa	$\phi = 41.46$ °	υ =0.21	c=150kPa	$\phi = 30$ °
-9		E_{solo} = 108MPa	Drucker-Prager		E_{solo} = 56 MPa	Drucker-Prager	
		$\upsilon = 0.27$	c=30 kPa	$\phi = 43.28$ °	υ =0.21	c=150kPa	$\phi = 30$ °
-10		E_{solo} =113.4Mpa	Drucker-Prager		E_{solo}=58.8MPa	Drucker-Prager	
		$\upsilon = 0.26$	c=30 kPa	$\phi = 43.98$ °	υ =0.21	c=150kPa	$\phi = 30$ °

5 RESULTS AND DISCUSSION

5.1 Analysis of variance

To verify the relevance of the various parameters the analysis of variance (ANOVA) was used across those numerical models analyzed.

In the analysis of variance developed in this work, fixed factors were used, where four study variables were chosen, those being the height of the pile cap (28 cm, 50 cm and 70 cm), the type of soil (absence of soil, sand and clay), the length of the piles (5 m, 7 m and 9 m), and the type of pile-soil bond (coupling of nodes and contact elements). With respect to the dependent variable, the ultimate strength of the models was used in one analysis and the percentage of force transferred to the ground directly through the pile cap in another analysis. In models without the presence of soil, the non-occurrence of geometric non-linearity was admitted, and the tip of the piles was considered as possessing a simple support. Due to the absence of soil, all vertical force was transferred directly to the tip of the piles and the block was able to move freely in the vertical direction. Noteworthy here is that the length of the piles was defined in order to obtain a variation in the rigidity of the system without having a high computational cost, since the models were simulated as in the presence of soil.

As the analysis of variance is indicated for samples that have a Normal distribution, a Shapiro-Wilk test [11] was performed to analyze the normality of the data. In addition to the Shapiro-Wilk test [11], an analysis was made of the Quantile-Quantile graph.

In Figure 10, the normality test referring to the ultimate strength data of models B2 (model without soil) and B3 (model with node coupling between pile and soil), as well as the normality test referring to the ultimate strength data of models B2 (model without soil) and B4 (model with the use of contact elements).

Thus, for the two simulations the data adjusted notably well to the normal distribution, however, the simulation between models B2 and B4 showed that the samples obtained with the introduction of contact elements had greater adherence to the Normal distribution.

Through Table 6, one notes that the analysis of the variational parameters was reached. If the P-value is less than the 0.05 significance level, the variable is considered relevant.

If the value of F-value is higher than the values of F-critical, provided by Montgomery [12], the parameter can be considered relevant within the analysis. When comparing the models without soil presence with the models for which the connection of the soil with the piles occurs through the coupling of nodes, the conclusion reached is that the variable S (soil type) has relevant importance in relation to the bearing capacity of the blocks followed by variable H (block height). Based on the values of F-value and P-value, the length of the pile (L) was shown as not being a parameter of great relevance, when compared to the type of soil and height of the block, the same goes for interaction between variables S and H, S and L and between variables H and L.
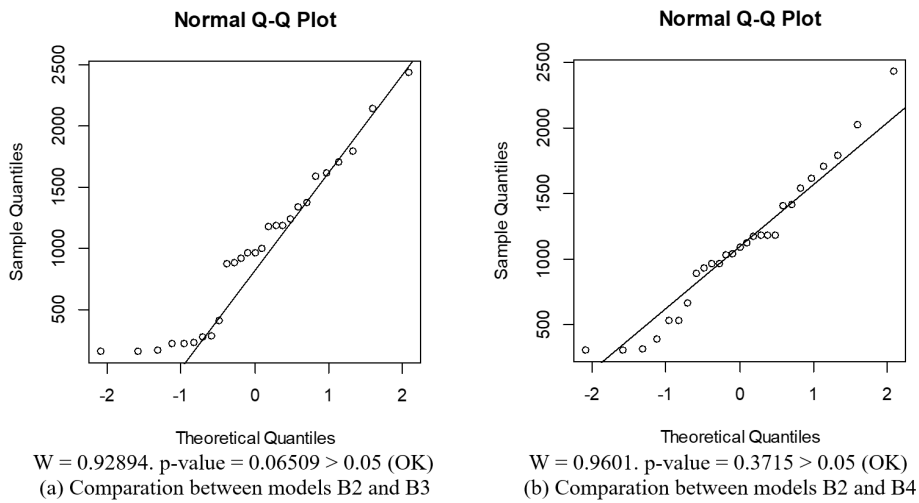
Rev. IBRACON Estrut. Mater., vol. 14, no. 6, e14604, 2021

10/19

Normal Q-Q Plot

W = 0.92894. p-value = 0.06509 > 0.05 (OK)
(a) Comparation between models B2 and B3

Normal Q-Q Plot

W = 0.9601. p-value = 0.3715 > 0.05 (OK)
(b) Comparation between models B2 and B4

Figure 10. Normality test for ultimate strength.

Table 7 presents the results of analysis of variance between the models without the presence of soil and the models in which the bond between soil and pile was through the contact elements. Similar to ANOVA, in which the ultimate strength was analyzed for models with knot coupling, it was found that the variable S greatly influences the carrying capacity of the models; however, the interaction between the variables S and H has no relevance in the analysis of parameters. The same occurred for the interactions between variables S and L and between variables H and L.

Table 6 – Analysis of variance of the ultimate force between models B2 and B3.

			Ultimate force (node coupling)			
Factors	Degrees of freedom	Sum of squares	Mean of squares	F-value	F-critical	P-value
S	2	7647491	3823745	65.15	3.40283	0.000
H	2	1488393	744197	12.68	3.40283	0.003
L	2	350747	175374	2.99	3.40283	0.107
S × H	4	642176	160544	2.74	2.92774	0.105
S × L	4	241892	60473	1.03	2.92774	0.448
H × L	4	81253	20313	0.35	2.92774	0.840
Error	8	469507	58688	-	-	-
Total	26	10921459	-	-	-	-

Table 7 – Analysis of variance of the ultimate force between models B2 and B4.

			Força última (Elementos de Contato)			
Factors	Degrees of freedom	Sum of squares	Mean of squares	F-Value	F-critical	P-Value
S	2	3916510	1958255	24.22	3.40283	0.000
H	2	3916510	497607	6.15	3.40283	0.024
L	2	774459	387230	4.79	3.40283	0.043
S × H	4	531922	132981	1.64	2.92774	0.254
S × L	4	435281	108820	1.35	2.92774	0.333
H × L	4	216620	54155	0.67	2.92774	0.631
Error	8	646806	80851	-	-	-
Total	26	7516813	-	-	-	-

In Figure 11, one notes, based on the average of the results, how the ultimate strength of the pile caps is influenced by varying the type of soil, the rigidity of the pile cap and the length of the pile. For the soil parameters used in the

Rev. IBRACON Estrut. Mater., vol. 14, no. 6, e14604, 2021

11/19

research, the higher level of stiffness in the sandy soil (S1) was noted in relation to the clayish soil (S2) and the superior strength of the models in which the soil is not considered. Noted also is that the increase in the height of the blocks directly influenced their bearing capacity, while generating greater impact when changing the parameter from 50 cm to 70 cm.

Regarding the length of the pile, there was noted for models with node coupling that on average the resistance of the models, for which the pile length is 7 meters (L7), was lower than for models with 5-meter piles, a fact that did not occur when simulating bonding by contact elements. For both analyzes the models with 9-meter piles had a much higher resistance.

To perform the analysis of variance for the percentage of force transferred directly to the soil through the pile cap, it was necessary to analyze whether the data have a normal distribution. Again, Shapiro-Wilk [11] and Quantile-Quantile plot methods were used. As seen from Figure 12, based on the P-value obtained, one is drawn to the conclusion that the data do not adhere to a Normal distribution. According to Gomes [13], if the data do not have a normal distribution, one can choose to treat and make them normal, where this is possible through the logarithmic transformations (log10) or through square root. The corroborators Santos et al. [14] obtained good adherence to the Normal distribution through a logarithmic transformation with base 10, obtaining a variation from $p < 0.05$ to $p > 0.10$ after the transformation. Therefore, in the present work, for the sample data of the percentage of force transferred to the soil through the block, the logarithmic transformation in base 10 was used as a data normalization tool. As identified in Figure 12, the transformation had an effect, ensuring the normality of the data.
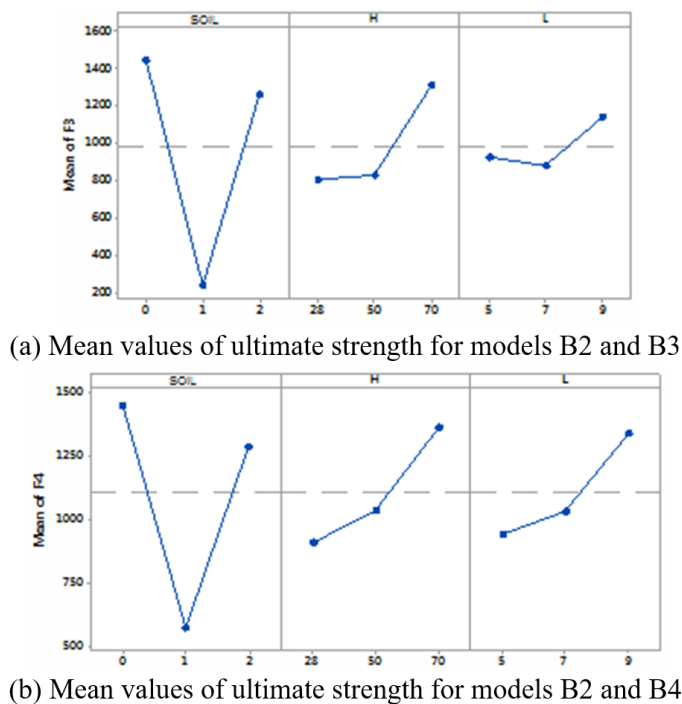

(a) Mean values of ultimate strength for models B2 and B3

(b) Mean values of ultimate strength for models B2 and B4

Figure 11. Parametric variation analysis, considering mean values of ultimate strength.

Table 8 shows the results of the analysis of variance for the portion of force transferred to the soil directly by the block, taking as variables the type of soil, the height of the block, the length of the piles and the type of piling-soil bonding.

Therefore, it is understood, through the analysis of the models, that the pile length (L) was the most relevant parameter, followed by the type of bond between the pile and the soil (coupling of nodes or contact elements) and the type soil (sand or clay). On the other hand, one recognizes that among the relevant parameters, the height of the block was the least relevant.
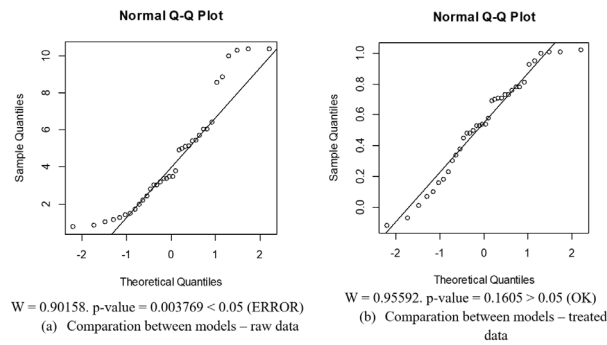
Figure 12. Normality test for data of percentage of force transferred to the ground through the pile-cap.

As shown in Figure 13, verification was made into how the interaction between the study variables influenced the percentage of force transferred from the block to the ground directly.

Table 8 – Analysis of variance about the percentage of force transferred to the soil through the pile cap.

| Factors	Degrees of freedom	Sum of squares	Mean of squares	F-Value	F-critical	P-Value
SOIL	1	0.30582	0.30582	**11.54**	**4.06705**	**0.004**
H	2	0.19866	0.09933	**3.75**	**3.21994**	**0.046**
L	2	1.84826	0.92413	**34.89**	**3.21994**	**0.000**
LINK	1	0.47998	0.47998	**18.12**	**4.06705**	**0.001**
SOIL × H	2	0.06251	0.03126	1.18	3.23810	0.333
SOIL × L	2	0.11072	0.05536	2.09	3.23810	0.156
SOIL × LINK	1	0.07144	0.07144	2.70	4.07855	0.120
H × L	4	0.05107	0.01277	0.48	2.63353	0.749
H × LINK	2	0.03050	0.01525	0.58	3.23810	0.574
L × LINK	2	0.03958	0.01979	0.75	3.23810	0.490
Error	16	0.42385	0.02649		-	
Total	35	3.62239			-	
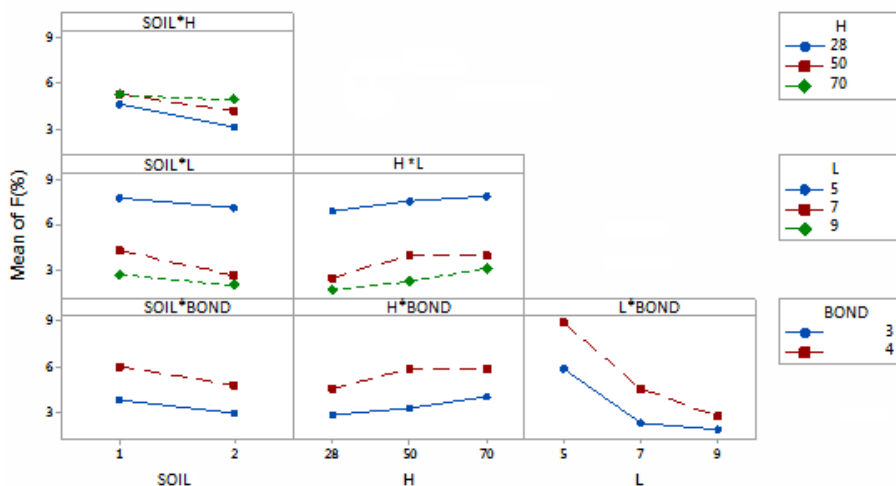
Figure 13. Interaction diagrams between control variables (Analysis between models B3 and B4) - Percentage of forces transferred to the ground through the pile-cap.

Regarding the interaction between the height of the block and the type of soil used in the study, it was found that for heights of 28 cm, 50 cm and 70 cm, the models with sandy soil transferred more force to the soil through the block, when compared to clayish soil, although, this discrepancy was less significant for blocks with a height of 70 cm. On the same graph it can be seen that the greater the block stiffness, the more significant the transfer of force from block to ground.

Another analysis performed corresponded to the interaction between the variables SOIL and L, as shown in Figure 13. It was found that for 9 m piles the load transfer to the soil through the block was lower than that of the models with a 7 m pile, which in turn was lower than that of the models with a 5 m pile. This is justified by the fact that the deeper layers of the soil have greater modulus of elasticity, therefore, being more rigid and having a greater tendency to absorb more activity than the more compressible layers, since the diameter of the piles and the material were fixed the same. It is important to note that this work, by itself theoretical, has chosen to adopt homogeneous behavior for the soil. Furthermore, in this work, the effect of the thickness of indescribable layers of soil and the effect of negative friction were not considered.

For the interaction between the types of bond with the type of soil, the same trend of less block-soil force transfer to the clay soil was noted. However, in the models in which a contact element was used, on average, a greater block-soil force transfer occurred. This fact is justified, as the coupling of nodes (bond 3) promotes a transfer of punctual forces through the piles (nodes coinciding between the pile and the soil), whereas in the models with contact elements (bond 4), this transfer occurs in a distributed way, according to relative displacements (displaceable model). As such, a greater rigidity of the soil pile set was noted in the models with knot coupling, creating in this way, greater force transference to the ground along the shaft.

The interaction between the height of the block and the length of the piles evidenced the reduction of force transferred to the soil through the block as the length of the pile increased. For the models with a 7 m pile, there was a tendency to stabilize the transferred force through increased rigidity of the block.

On the topic of the behavior of the models when analyzing the height of the block and the types of bond, little relevance was found in the analysis. An increase in the transferred force is perceived by increasing the stiffness for both types of bonding; however, this increase was not significant.

Finally, the interaction between the length of the piles and the type of piling-soil bonding was analyzed, the conclusion was thus reached that the variation of the transferred force, by increasing the length of the piles, was relevant and led to a tendency of stabilization by increasing the length of the pile. This fact was evident both for models with nodes coupling (bond 3), as well as for models in which contact elements were used (bond 4).

5.2 Force-displacement analysis

In this section, the force-displacement results for the analyzed models are presented. Through this analysis, the variation in the rigidity of the models can be identified, based on the support condition (bonding), block height, pile support level and soil type.

As seen from Figure 14, when taking into account the length of the pile, it was found that, in the models in which there is soil (S1 or S2), the support dimension of the pile influenced the overall stiffness of the model.

Verified also was the greater rigidity of the models without the presence of soil, since such models have as a boundary condition, the zero-vertical displacement. It is important to mention that, in models with no soil (S0), a reduction in stiffness was noted due to the increase in pile length. This is justified by the fact that the pile deformation is linked to its axial stiffness (constant for all piles) and its length (variable).

Through Figure 14, it is also possible to analyze the influence of the type of soil on the ultimate strength of the models. In (a), (b) and (c), force-displacement graphs are noted for models without soil (S0) and sandy soil (S1) and in (d), (e) and (f), the force-displacement graphs for models without soil (S0) and clay soil (S2). For the types of soil profiles adopted in the study, there was greater stiffness noted for the sandy soil, since it presented a lower settlement for the same applied force, in comparison to the clayish soil. This in turn, due to the set of parameters adopted (cohesion, modulus of elasticity, Poisson's ratio and friction angle), made the obtainment of a greater load capacity possible.

In terms of the type of bonding, those models simulated with sandy soil, along with the use of contact elements were found to show a higher bearing capacity and greater deformability, when compared with the models simulated with knot coupling. This discrepancy in results was not widely observed for clayish soils. It was found that, although the models with contact elements are more deformable and have a higher bearing capacity, the behavioral tendency of the models with coupling nodes (B3) and contact elements (B4) was similar.
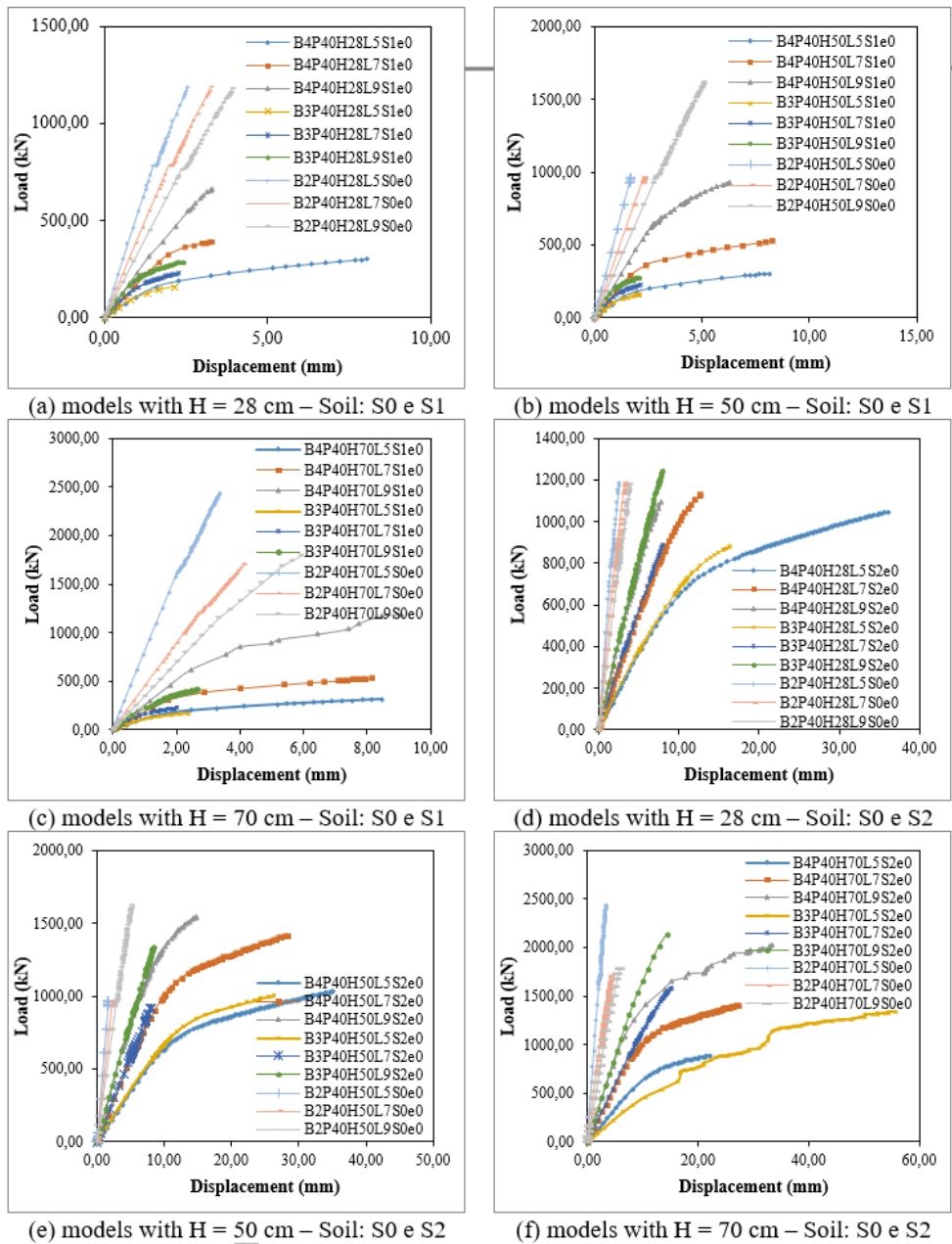
Figure 14. Graphics load-displacement of the analyzed models

5.3 Main compression stress

This session presents the results of the main compression stress on concrete blocks, obtained through numerical analysis. In Figure 15, the formation of the compressed diagonals is noted. Highlighted here was that in all models, the highest stress was noted as developing in the upper nodal region, a fact that was also observed by Munhoz [15] and Delalibera [6].

Regarding the field of stress, this was seen, through analysis, to have the tendency to form beyond the column section, contradicting the hypothesis proposed by Blévot and Frémy [2]. In models B1P40H28 and B2P40H28, in the lower nodal region, an expansion of the stress field beyond the external region of the piles was observed, as noted from Figure 15. This fact was not observed in the models B3P40H28 and B4P40H28.
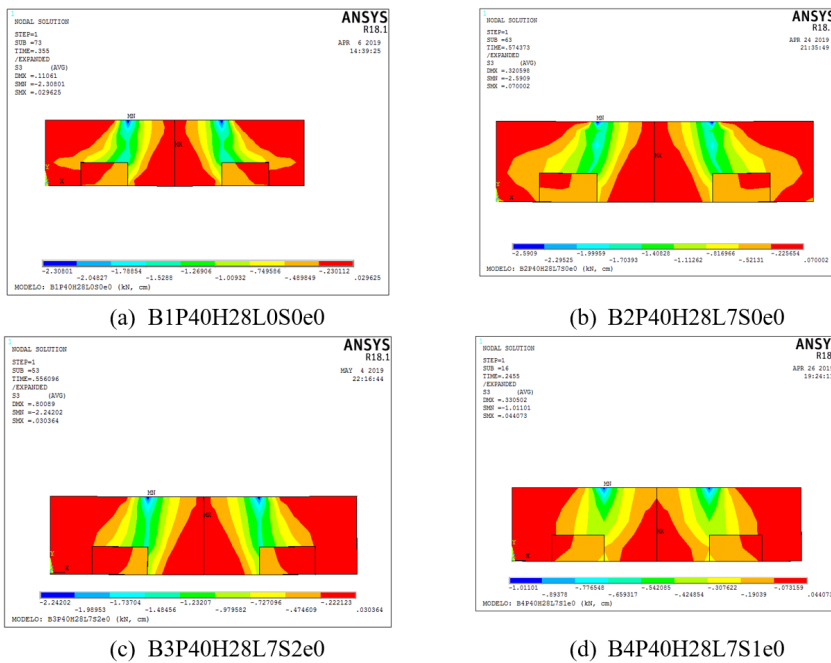
(a) B1P40H28L0S0e0

(b) B2P40H28L7S0e0

(c) B3P40H28L7S2e0

(d) B4P40H28L7S1e0

Figure 15. Main compression stresses in the pile-caps

In the models with H50 and H70, the expansion in the stress field in the lower nodal region occurred similarly to that in models B2, B3 and B4, where the expansion in the stress field in the regions outside the piles is observed, as shown in Figure 16. Emphasis is here placed on the fact that for all models with blocks of height 50 and 70 cm, the expansion of the stress field in the lower nodal region occurred in a similar way.

Another aspect for consideration refers to the fact that, in the sandy soil models (S1), the stresses acting on the blocks were below the fracture limits, this fact occurred due to the greater rigidity of the constitutive model of the studied sandy soil, causing the model to lose stability for lower forces more than expected.

Variations of the main compression stresses acting in the top of the piles were also verified.
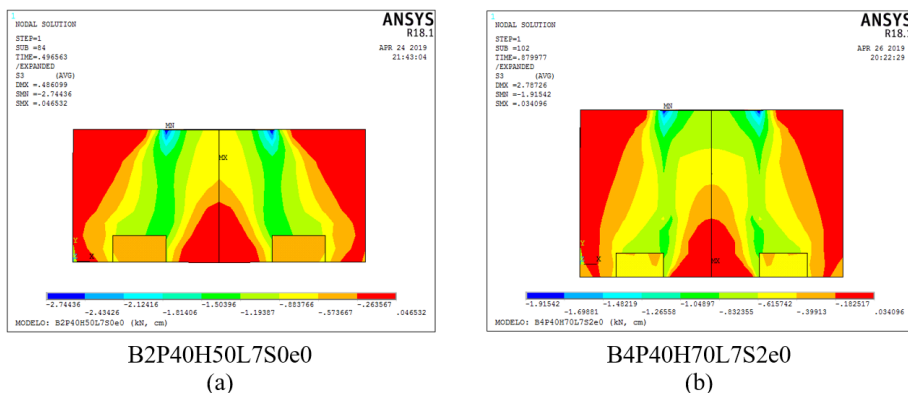

B2P40H50L7S0e0
(a)

B4P40H70L7S2e0
(b)

Figure 16. Main compression stresses in the pile-caps

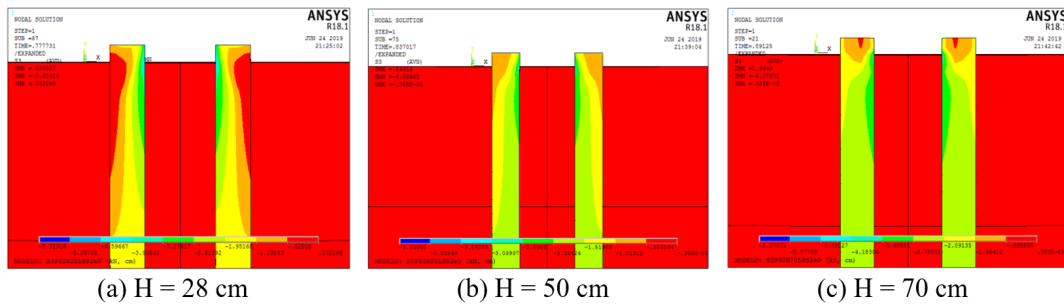(a) H = 28 cm   (b) H = 50 cm   (c) H = 70 cm

Figure 17. Main compression stresses in the piles

As seen in Figure 17, although the pillar is being exposed only by vertical compression force, the piles were exposed to flexion-compression. This effect proved to be more significant in blocks with a height of 28 cm, due to the lower rigidity of the model and greater tendency for flexion to occur. The reduced effect of flexion-compression in models with a height of 50 cm and 70 cm is noted in Figure 17, where there was less variation in the stress field, revealing the occurrence of a lesser effect from the bending moment on the top of the piles.

5.4 Settlement Analysis

The comparative analysis between settlements in piles obtained numerically with the ANSYS® software [3] and those obtained according to the method of Poulos and Davis [16] increased, due to the group effect, which is in agreement with the method proposed by Fleming et al. [17], and Equation 4 is found on Table 9.

$$\text{Increase factor of settlement} = n^k \tag{4}$$

In this context, n is the number of piles and k is a constant that varies between 0.40 and 0.60.

Table 9 – Comparison between settlements obtained numerically and analytically.

Model	Displ. numerical R_N (mm)	Displ. analytical R_A (mm)	R_A / R_N	Model	Displ. numerical R_N (mm)	Displ. analytical R_A (mm)	R_A / R_N
B3P40H28L5S1e0	2.14	2.09	0.98	B4P40H28L5S1e0	8.05	3.96	0.49
B3P40H28L7S1e0	2.28	1.13	0.50	B4P40H28L7S1e0	3.31	1.92	0.58
B3P40H28L9S1e0	2.41	0.87	0.36	B4P40H28L9S1e0	3.30	2.01	0.61
B3P40H50L5S1e0	2.12	2.11	1.00	B4P40H50L5S1e0	8.17	4.00	0.49
B3P40H50L7S1e0	2.13	1.12	0.53	B4P40H50L7S1e0	8.27	2.59	0.31
B3P40H50L9S1e0	2.07	0.42	0.20	B4P40H50L9S1e0	6.30	2.84	0.45
B3P40H70L5S1e0	2.37	2.20	0.93	B4P40H70L5S1e0	8.47	4.08	0.48
B3P40H70L7S1e0	1.99	1.09	0.55	B4P40H70L7S1e0	8.17	2.59	0.32
B3P40H70L9S1e0	2.66	1.25	0.47	B4P40H70L9S1e0	9.07	3.59	0.40
B3P40H28L5S2e0	16.33	20.02	1.23	B4P40H28L5S2e0	36.08	23.77	0.66
B3P40H28L7S2e0	8.01	7.45	0.93	B4P40H28L7S2e0	12.68	9.45	0.75
B3P40H28L9S2e0	7.94	6.05	0.76	B4P40H28L9S2e0	7.76	5.32	0.69
B3P40H50L5S2e0	26.29	22.83	0.87	B4P40H50L5S2e0	35.23	23.50	0.67
B3P40H50L7S2e0	7.97	7.70	0.97	B4P40H50L7S2e0	28.30	11.88	0.42
B3P40H50L9S2e0	8.44	6.51	0.77	B4P40H50L9S2e0	14.79	7.50	0.51
B3P40H70L5S2e0	75.19	31.19	0.41	B4P40H70L5S2e0	22.03	20.22	0.92
B3P40H70L7S2e0	15.25	13.35	0.88	B4P40H70L7S2e0	27.38	11.79	0.43
B3P40H70L9S2e0	14.44	10.40	0.72	B4P40H70L9S2e0	33.52	9.86	0.29

The numerical models were verified by use of the soil parameters, as such the displacements were shown to be superior to the displacements obtained analytically by the method of Poulos and Davis [16], even when considering the

increase in repression due to the group effect. In general, in the models in which bonding by contact elements was considered (B4), there was a discrepancy between the numerical and analytical models. In the models with sandy soil (S1) in which the bond was made by knot coupling (B3), it was found that the shorter the pile length, the greater the agreement between the numerical method and the analytical method. In general, the numerical models with node coupling bond presented a better agreement with the analytical method, representing with greater consistency the repression in the models.

6 CONCLUSIONS

By taking into consideration both the main compression stresses and the formation of compressed diagonals, in the upper nodal region the strut and tie model was understood to form beyond the column section, contrary to the hypothesis proposed by Blévot and Frémy [2]. In the pile cap models with a height of 28 cm and with no soil, there was an expansion of the stress field in the lower nodal region beyond the external region of the piles, a fact also noted in the models of the same height, with soil presence. In models for which pile caps have a height of 50 cm and 70 cm, the expansion in the stress field in the lower nodal region occurred in similar fashion across models B2, B3 and B4. This was a fact highlighted more emphatically in the rigidity of the models in which the presence of sandy soil was considered (S1). In these models, due to the adopted soil parameters, the stresses acting on the pile caps were lower than the fracture limits, this occurred due to the fragility that was established in the sandy soil constitutive model, causing the system to lose numerical stability for forces lower than expected.

There was a tendency of flexion-compression occurring within the tops of the piles, therefore, verifying the piles and allowing that these be only subject to the normal compression force can lead to results not consistent with the real behavior of the structure, mainly for blocks with low stiffness. In the present research, the increase in the block stiffness was noted as leading to a reduction in the variation in the field of main compression stresses at the top of the piles, demonstrating that the increase in the pile cap stiffness has a favorable effect regarding the transfer of bending moments to the piles.

Considering the global stiffness of the models, in terms of the soil profiles adopted, the support level of the piles can be considered as a direct influence on this parameter, since, with an increase in the depth of the soil, the stiffness increases, and the deformability of the soil is reduced. Therefore, the result of increased rigidity by increasing the support quota is consistent. The models with no soil showed greater rigidity, however, still showing variation in displacement due to the variation in the length of the piles. This was justified by the fact that the axial rigidity of the pile is constant, and the deformation of the pile is directly proportional to its length. On average, the increase in the height of the models led to an increase in their ultimate strength.

Regarding the transfer of force to the soil through the block, it was found that for soil with sandy characteristics, the average transfer is approximately 5% of the total applied force, while for clay soils this value is close to 4%. It was also found that the increase in the rigidity of the pile cap provided, on average, an increase in the transfer of force from the pile cap to the ground. As for the length of the piles, once parameters such as diameter and material of the piles were fixed, the stiffness of the soil in the pile settlement level was noted as directly influencing the percentage of force transferred from the pile cap to the soil. Due to the aforementioned, the conclusion was reached that the more rigid soil-pile systems tended to transfer less force to the soil through the pile cap. This conclusion highlights the tendency for the force to be distributed primarily to regions of greater rigidity.

For the interaction between the types of bond with the type of soil, there was noted for the models in which contact element was used, on average, a greater block-soil transfer of force occurred. This fact is justified by the fact that the coupling of nodes promoted a transfer of punctual forces through the piles (nodes coinciding between the pile and the soil) whereas in the models with contact elements, this transfer occurs in a distributed manner, according to relative displacements (more displaceable model). A greater rigidity of the pile-soil set was thus noted in the models with node coupling, causing more force to be transferred to the soil along the shaft.

One can also conclude that to analyze the repression in the piles, the knot-coupling bond tends to represent more realistically the analytical model of Poulos and Davis. Added to this was a filter referring to the length of the piles, since it was evident, for sandy soils, that the shorter the length of the piles, the better the agreement between the settlements obtained numerically and those obtained analytically through the method of Poulos and Davis [16] and Fleming et al. [17].

7 ACKNOWLEDGMENTS

8 REFERENCES

[1] Associação Brasileira de Normas Técnicas, *Design of Concrete Structures – Procedure*, NBR 6118, 2014.

[2] J. Blévot and R. Frémy, "Semelles sur piex," *Analles Inst. Techique Batiment Trav. Publics Paris*, vol. 20, no. 230, pp. 223–295, 1967.

[3] Ansys, Inc., *ANSYS 2020 R2: Theory Manual.* Canonsburg, PA: ANSYS, 2020.

[4] K. J. Willam and E. P. Warnke, "Constitutive model for triaxial behavior of concrete," in *Proc. Int. Assoc. Bridge Struct. Eng. Conf.*, 1974, pp. 174–191.

[5] P. Desay and S. Krishnan, "Equation for the stress-strain curve of concrete, ACI Journal," *Proc.*, vol. 61, no. 3, pp. 345–350, 1964.

[6] R. G. Delalibera, "Numerical and experimental analysis of pile caps with two piles submitted to axial and eccentric forces," Ph.D. dissertation, Sch. Eng. São Carlos, São Paulo Univ., São Carlos, 2006 (in Portuguese).

[7] F. S. Munhoz, "Experimental and numerical analysis of rigid blocks on two piles with pillars of square and rectangular sections and different reinforcement rates," Ph.D. dissertation, Sch. Eng. São Carlos, São Paulo Univ., São Carlos, 2014.

[8] G. H. Silva, "Choice of parameters for contact analysis between elastic bodies using finite elements and neural networks," M.S. thesis, FEC, UNICAMP, Campinas, 2009.

[9] NAVFAC, *Design Manual. 7.02, Foundations & Earth Structures.* Alexandra, VA: Dept. Navy, Nav. Facil. Eng. Command, 1986.

[10] J. C. A. Cintra and N. Aoki, *Fundation for Piles: Geotechnical Project*. São Paulo: Oficina de Textos, 2010.

[11] S. S. Shapiro and M. B. Wilk, "An analysis of variance test for normality (complete samples)," *Biometrika*, vol. 52, pp. 591–611, 1965.

[12] D. C. Montgomery, *Design and Analysis of Experiments*, 4th ed. New York: John Wiley & Sons, 1996.

[13] P. S. Gomes, "Asymmetric normal distribution for gene expression data," Ph.D. dissertation, Fed. Univ. São Carlos, São Carlos, 2009.

[14] J. O. Santos, C. S. Munita, C. Vergne, and P. M. S. Oliveira, "Standardization and standardization through logarithmic transformation in archeometric studies of ceramics," in *52ª RBras*, 2007, pp. 1–5. Accessed: Apr. 29, 2019. [Online]. Available: https://www.ipen.br/biblioteca/2007/eventos/13990.pdf

[15] F. S. Munhoz, "Analysis of the behavior of reinforced concrete blocks on piles subjected to the action of centered force," Ph.D. dissertation, Sch. Eng. São Carlos, São Paulo Univ., São Carlos, 2004.

[16] H. G. Poulos and E. H. Davis, *Pile Foundation Analysis and Design*. New York: Wiley, 1980.

[17] W. G. K. Fleming, A. Weltman, M. Randolph, and W. Elson, *Pile Engineering*. Glasgo, Scotland: Blackie & Son, 1985.